Published in final edited form as:

Circulation. 2020 July 21; 142(3): 259–274. doi:10.1161/CIRCULATIONAHA.119.044452.

The Role of Non-Glycolytic Glucose Metabolism in Myocardial Recovery upon Mechanical Unloading and Circulatory Support in Chronic Heart Failure

Rachit Badolia, PhD[1,2], **Dinesh K. A. Ramadurai, B.Tech**[1], **E. Dale Abel, MD, PhD**[3], **Peter Ferrin, BA**[1], **Iosif Taleb, MD**[1,2], **Thirupura S. Shankar, B.Tech**[1], **Aspasia Thodou Krokidi, MS**[1], **Sutip Navankasattusas, PhD**[1], **Stephen H. McKellar, MD**[2], **Michael Yin, MD**[2], **Abdallah G. Kfoury, MD**[2], **Omar Wever-Pinzon, MD**[2], **James C. Fang, MD**[2], **Craig H. Selzman, MD**[1,2], **Dipayan Chaudhuri, MD, PhD**[1], **Jared Rutter, PhD**[4], **Stavros G. Drakos, MD, PhD**[1,2]

[1]Nora Eccles Harrison Cardiovascular Research and Training Institute, University of Utah, Salt Lake City, Utah, USA

[2]U.T.A.H. (Utah Transplant Affiliated Hospitals) Cardiac Transplant Program: University of Utah Healthcare and School of Medicine Intermountain Medical Center, Salt Lake VA (Veterans Affairs) Health Care System, Salt Lake City, Utah, USA.

[3]Division of Endocrinology, Metabolism and Diabetes and Fraternal Order of Eagles Diabetes Research Center, Carver College of Medicine, University of Iowa, Iowa City, Iowa, USA.

[4]Department of Biochemistry, University of Utah and Howard Hughes Medical Institute (HHMI), Salt Lake City, Utah, USA

Abstract

Background: Significant improvements in myocardial structure and function have been reported in some advanced heart failure (HF) patients (termed Responders-R) following left ventricular assist device (LVAD)-induced mechanical unloading. This therapeutic strategy may alter myocardial energy metabolism in a manner that reverses the deleterious metabolic adaptations of the failing heart. Specifically, our prior work demonstrated a post-LVAD dissociation of glycolysis and oxidative-phosphorylation characterized by induction of glycolysis without subsequent increase in pyruvate oxidation via the TCA cycle. The underlying mechanisms responsible for this dissociation are not well understood. We hypothesized that the accumulated glycolytic intermediates are channeled into cardioprotective and repair pathways, such as the pentose-phosphate pathway and one-carbon metabolism, which may mediate myocardial recovery in Responders.

Methods: We prospectively obtained paired LV apical myocardial tissue from non-failing donor hearts as well as responders and non-responders at LVAD implant (Pre-LVAD) and transplantation

ADDRESS FOR CORRESPONDENCE Stavros G. Drakos, MD, PhD, FACC, Stavros.Drakos@hsc.utah.edu, Address: Nora Eccles Harrison Cardiovascular Research and Training Institute (CVRTI), 95 South 2000 East, Salt Lake City, UT 84112-5000, Phone: 801-587-9533, Fax: 801-581-3128.

CONFLICT OF INTEREST DISCLOSURES

Dr. Drakos is a consultant to Abbott and receives research support from Merck.

(Post-LVAD). We conducted protein expression and metabolite profiling and evaluated mitochondrial structure using electron microscopy.

Results: Western blot analysis shows significant increase in rate-limiting enzymes of pentose-phosphate pathway and one-carbon metabolism in Post-LVAD responders (Post-R) as compared to post-LVAD non-responders (Post-NR). The metabolite levels of these enzyme substrates, such as sedoheptulose-6-phosphate (pentose phosphate pathway) and serine and glycine (one-carbon metabolism) were also decreased in Post-R. Furthermore, Post-R had significantly higher NADPH levels, reduced ROS levels, improved mitochondrial density and enhanced glycosylation of the extracellular matrix protein, α-dystroglycan, all consistent with enhanced pentose-phosphate pathway and one-carbon metabolism that correlated with the observed myocardial recovery.

Conclusions: The recovering heart appears to direct glycolytic metabolites into pentose-phosphate pathway and one-carbon metabolism which could contribute to cardioprotection by generating NADPH to enhance biosynthesis and by reducing oxidative stress. These findings provide further insights into mechanisms responsible for the beneficial impact of glycolysis induction during the recovery of failing human hearts following mechanical unloading.

Keywords

Heart Failure; LVAD; MCS; Glucose metabolism; Pentose phosphate pathway; One-Carbon metabolism; Reverse remodeling; Myocardial recovery

INTRODUCTION

Heart Failure (HF) is a global epidemic causing a huge financial burden on the healthcare system. Mortality rates exceed 50% in patients with advanced HF. Mechanical unloading through LVAD is a therapeutic intervention which serves either as a bridge to heart transplant or destination/lifetime therapy. Multiple studies reveal that LVAD unloading and circulatory support leads to substantial cardiac function improvement in a subgroup of patients (Responders) with end-stage HF [1-3].

Metabolism is inextricably linked with cardiac function and is tightly regulated [4, 5]. Oxidation of fatty acids, glucose and lactate in mitochondria accounts for most of the ATP generation in healthy adult hearts, with fatty acids being the preferred energy substrate, providing > 70% of the total ATP [5]. Altered energetics and metabolic reprogramming are believed to be integral to HF development and progression with the failing heart exhibiting a “fetal pattern” of substrate utilization characterized by enhanced glycolysis and decrease in fatty acid oxidation [4, 6]. It was suggested that LVAD-induced unloading has the potential to reverse the deleterious metabolic adaptations of the failing heart and even activate cellular pathways of cardioprotection and cardiac repair [7-9]. The mechanisms by which LVAD-induced mechanical unloading affects the energy balance and metabolic reprogramming of chronic HF is not well understood. We reported in our previous study that the levels of glycolytic intermediates were induced post-LVAD, however most of the pyruvate was not directed to the Tricarboxylic acid (TCA) cycle [7]. The absence of a corresponding increase in the intermediates of the TCA cycle and electron transport chain activity in mitochondria strongly suggested a glycolysis-oxidative phosphorylation mismatch during mechanical

unloading [7]. This may be, in part, due to the decreased myocardial energy demand during unloading/ 'resting' making glycolysis a sufficient energy source. Alternatively, this could be explained by the channeling of glucose to the accessory metabolic pathways (**outlined in** Figure1) such as the pentose phosphate pathway and one-carbon metabolism, following LVAD support.

The first step of the pentose phosphate pathway is oxidation of glucose-6-phosphate (a product of glycolysis) via activity of the rate-limiting enzyme glucose-6-phosphate dehydrogenase (G6PD) using NADP+ (Figure 1). The pentose phosphate pathway generates NADPH, an important electron donor for reductive biosynthesis and for defense against reactive oxygen species (ROS) [10]. Pentose sugars produced in the pathway can also be converted to ribitol, which is essential for the glycosylation of α-dystroglycan (α-DAG1) [11]. The interaction of α-DAG1 with extracellular matrix proteins is critical for maintaining muscle integrity and function [11, 12]. The one-carbon metabolism pathway derived from 3-phosphoglycerate by the activity of phosphoglycerate dehydrogenase (PHGDH) is a major contributor for purine synthesis and generation of NADPH in the cytosol and mitochondria (Figure 1) [13, 14]. Hence, the pentose phosphate pathway and the one-carbon metabolism pathway lead to an inherent coupling of nucleotide synthesis with NADPH production [13]. Alternatively, glucose-derived metabolites may enter the polyol pathway through glucose-6-phosphate and into the hexosamine biosynthetic pathway through fructose-6-phosphate. Although glycolysis and glucose oxidation are the pathways whereby glucose metabolism is optimized for ATP production, these accessory pathways play critical roles in biomass accumulation, ROS defense and cell regulation.

In this study, we investigated these accessory pathways of glucose metabolism in responders and non-responders after LVAD-induced mechanical unloading. We show that myocardial recovery correlates with the increased shunting of glycolytic intermediates into accessory pathways such as the pentose phosphate pathway and one-carbon metabolism, to generate biomolecules that support repair and maintain the redox status of cardiomyocytes.

METHODS

Disclosure:

The authors declare that all supporting data are available within the article (and its online supplementary files).

Study Population

Patients with advanced HF were prospectively enrolled at the time of LVAD implant as a bridge-to-transplant or destination therapy. Patients who received LVAD secondary to acute HF were prospectively excluded. Control tissue was acquired from Donors with non-failing hearts that were not allocated for transplantation due to non-cardiac reasons. This study was carried out at institutions comprising the UTAH Cardiac Transplant Program (University of Utah Health Science Center, Intermountain Medical Center, and the George E. Wahlen VA Medical Center, Salt Lake City, Utah). The institutional review board of each institution approved the study and all patients provided informed consent.

Clinical Data Collection

We collected clinical data including demographics, comorbidities, invasive hemodynamic and laboratory information within 1 week before LVAD implantation and again between 2-4 weeks after device implantation. Structural and functional response to unloading was determined via serial 2-dimensional, M-mode, and Doppler echocardiograms that were performed monthly. Additionally, before LVAD implantation, baseline transthoracic echocardiograms were taken. We followed the serial echocardiographic data of patients after surgery for up to 6 months and, based on the two key parameters during diminished support or “turn-down” echo’s: LVEF and LVEDD, they were categorized as either responder or non-responder. These echocardiographic parameters were measured after 30 minutes of diminished LVAD support, i.e. “turn-down” echos. Specifically, the revolutions per minute of the LVAD device were reduced for 30 min to the minimum allowed by the manufacturer in order to increase the load on the myocardium. Responders (R) were defined as having a relative increase in left ventricular ejection fraction (LVEF) ≥ 50% compared to baseline, a final resulting EF≥ 40%, and a final left ventricular end diastolic diameter (LVEDD) of <6 cm. If these criteria were not met, the patient was considered a Non-Responder (NR). The phenotypic status of the patients was determined only if patients had undergone at least a minimum of 3 months of LVAD support, given prior work by us and others that this represents the minimum time on support to attest for potential salutary effects of mechanical unloading and circulatory support induced by LVAD.

Tissue Acquisition

Myocardial tissue was acquired from organ donors and consenting HF patients as described previously [7].

Materials

Antibodies to G6PDH (#8866), Transketolase (#8616), PHGDH (#13428), SHMT2 (#12762), Catalase (#12980), SOD1 (#4266), GPX1 (#3206), PRDX2 (#46855), GLUT1 (#12939), GLUT4 (#2213), GFAT1 (#3818), O-GlcNAc (#9875), Ribosomal protein L7a (#2415), Ribosomal protein S3 (#9538) were obtained from Cell Signaling Technology (Beverly, MA). Antibodies to HSP60 (#MA3-012), and ISPD (#PA5-25854) from Thermo Fisher (Waltham, MA); FKRP (#sc-374642), TALDO (#sc-365449) and ALDR (#sc-166918) from Santa Cruz Biotechnology (Santa Cruz, CA); Anti-4HNE (#46545) from Abcam (Cambridge, MA) and; α-Dystroglycan (IIH6C4) (#05-593) from EMD Millipore (Burlington, MA). Amersham Protran 0.45 μM nitrocellulose membrane (#10600003) and ECL Prime western blotting detection reagent (#RPN2232) from GE Healthcare Life Sciences (Germany). LI-COR Odyssey blocking buffer, IRDye 680RD Donkey anti-mouse (#926-68072) and, IRDye 800CW Donkey anti-rabbit (#926-32213) from LI-COR (Lincoln, NE). NADP/ NADPH Assay kit (#ab176724) from Abcam (Cambridge, MA) and OxyBlot Protein Oxidation Detection kit (#S7150) from Millipore Sigma (Darmstadt, Germany).

Metabolomic analysis

The levels of metabolites in cardiac tissue were quantified by gas chromatography–mass spectroscopy (GC-MS) analysis, as described previously[7].

Western Blot analysis

Proteins were extracted using RIPA lysis buffer containing HALT Protease and Phosphatase inhibitor cocktail solution (Pierce, Rockford, IL). After homogenization using a bead-homogenizer, tissue lysates were incubated on ice for an hour. Samples were centrifuged at 14,000g for 30 minutes at 4^0C. Equal volume of 2X sample buffer containing 1 mM DTT was added to the supernatant. Protein estimation was performed using Pierce BCA Protein Assay Kit (Thermo Scientific, Rockford, IL). Samples were boiled for 10 minutes and 30 μg of protein was loaded on 8-12% SDS-PAGE gels. SDS-PAGE and western blotting was performed.

Electron Microscopy:

Epon-embedded tissue blocks were subjected to ultramicrotomy and osmium/uranyl acetate-based staining for electron microscopy. Imaging was performed on a JEM 1010 electron microscope (Jeol, Peabody, Massachusetts). A total of 5 optical fields/ heart were examined at 11,000 x magnification. Mitochondrial number and volume density were estimated as previously described[7].

NADP/NADPH Assay

50 mg tissue samples were washed with cold PBS and homogenized in 400 μl of mammalian cell lysis buffer using a bead homogenizer (20 Hz for 2-4 minutes). Homogenates were centrifuged at 2500 RPM for 10 mins at room temperature. Supernatants were transferred in a new tube and the NADPH/ NADP assay was performed following manufacturer's instructions (Abcam, Cambridge, MA). Fluorescence was measured in a microplate reader at Excitation/Emission =540/590.

Statistics

Statistical analysis was performed using GraphPad Prism software. Measures of variation were expressed as mean ± standard error of the mean. Significant differences were determined using either Student's *t*-tests (two-tailed) for 2 independent samples or using ordinary one-way ANOVA test (corrected for multiple comparisons with Tukey) for all groups. Multiple t-test was performed for nucleotides levels and two-way ANOVA for mitochondrial size. p-value < 0.05 was considered statistically significant.

For the clinical table, descriptive statistics were used, including frequencies, percentages and means. Measures of variation were expressed as mean ±standard error and compared using the student's t-test for independent samples. Categorical data were compared using the χ^2 test or Fisher's exact test, as appropriate. Univariate analyses were performed to determine the effect of baseline variables on the phenotypic status of the patients. A 2-tailed p value <0.05 was considered statistically significant. Analyses were performed by using SPSS version 20.0 (SPSS Inc, Chicago, IL).

Study Approval

The study was approved by the University of Utah's Institutional Review Board (IRB_00030622) entitled "Effects of Mechanical Unloading on Myocardial Function and

Structure in Humans". No study-related procedure was done before obtaining signed consent forms from all patients or their representatives. All the procedures followed were in accordance with institutional guidelines.

RESULTS

Study population and clinical characteristics

Consecutive patients with advanced HF were evaluated at the time of LVAD implantation and clinical characteristics of study subjects are shown in Table 1. LVEF and LVEDD were measured using turn-down echocardiography before and after the LVAD implantation as described in the method section. Patients with a post-LVAD LVEF ≥40% along with a >50% relative LVEF improvement and a LVEDD <6 cm were classified as responders, whereas patients with LVEF <35% or a relative improvement of LVEF <50% (regardless of LVEDD) as non-responders [15]. The responders had significantly higher mean LVEF of 42.2±2% after LVAD support as compared to the non-responders whose mean LVEF was 19.3±1%, despite having similar LVEF prior to LVAD implant. The LVEDD after LVAD implant was significantly lower in responders (4.8±0.4 cm) than the non-responders (6.3±0.2 cm). The responders also had higher prevalence of non-ischemic cardiomyopathy and they were significantly younger with shorter duration of HF symptoms.

Changes in Glucose uptake, Polyol and Hexosamine biosynthetic pathways in relation to cardiac recovery.

Glucose enters the cardiac myocyte via the insulin-sensitive glucose transporter 4 (GLUT4) and the insulin-independent GLUT1. GLUT4 is the major transporter given its greater abundance and translocation to the sarcolemma in response to cardiac contraction. GLUT4 expression decreases in HF and cardiac hypertrophy while GLUT1 is elevated in cardiac hypertrophy [16]. We investigated protein abundance of glucose transporters using paired myocardial tissue samples obtained at the time of LVAD implantation (pre-LVAD) and at time of transplantation (post-LVAD) from both responders (R) and non-responders (NR). Figure 2A and 2B shows similar levels of GLUT4 across the various groups. Relative to donor hearts, post-LVAD hearts from both R and NR shows a significant increase in GLUT1 protein (Figure 2A and 2C), suggesting enhanced glucose uptake upon mechanical unloading.

Glucose can be metabolized in multiple pathways providing not only ATP but also important metabolites for cellular functions. Glucose-6-phosphate generated during glycolysis can be converted to sorbitol via aldose reductase (ALDR) in the polyol pathway (Figure 1). Using the metabolomic analysis, we discovered that the levels of sorbitol are significantly lower in Post-R hearts relative to donor and Post-NR (Figure 2D). It was previously reported that ALDR expression was induced by two-fold in failing human hearts [17]. However, the levels of ALDR in this study appear to be similar among the failing and non-failing hearts, with a significant reduction in Post-R relative to the Post-NR (Figure 2E-2F). Given the reduction in ALDR in Post-R, it is possible that reduced sorbitol in Post-R could be due to decreased flux toward sorbitol synthesis, suggesting downregulation of polyol pathway in post-LVAD responders.

Glucose also supports flux into the hexosamine biosynthetic pathway via the activity of the rate-limiting enzyme, glutamine fructose-6-phosphate amidotransferase (GFAT), which converts the glycolytic intermediate fructose-6-phosphate to the principal end product uridine diphosphate-N-acetylglucosamine (UDPGlcNAc) (Figure 1). UDPGlcNAc is the substrate for O-linked glycosylation of a number of proteins via transferases [18] and hence an increase in hexosamine biosynthetic pathway flux may promote protein O-linked β-N-acetylglucosamine glycosylation (O-GlcNAcylation). Multiple studies reported increased mRNA and protein for O-linked β-N-acetylglucosamine transferase (GFAT) and increased UDPGlcNAc levels in mouse models of heart failure and hypertrophy [19, 20]. Western blot analysis of GFAT1 protein revealed similar protein levels across the various groups, with no difference between Post-NR and Post-R (Figure 2G and 2H). Interestingly, despite similar enzyme levels, the O-GlcNAcylation of proteins (using a specific antibody for O-GlcNAc) revealed a significant increase in O-GlcNAcylation of proteins in Post-NR compared to Donors (Figure 2G and 2I). Glycosylation in Post-R was significantly reduced as compared to Post-NR (Figure 2G and 2I), suggesting increase flux into hexosamine biosynthetic pathway specifically in Post-NR.

Pentose phosphate pathway and myocardial recovery

To examine potential contributions of the pentose phosphate pathway to myocardial recovery, we examined protein abundance of key enzymes and metabolites (Figure 1) involved in this pathway. Western blot analysis showed a trend towards an increase in G6PD, transketolase (TKT), and transaldolase (TALDO) in the failing heart (Pre-R and Pre-NR) relative to donors (Figure 3A-3D), supporting prior reports in animal models of HF [21, 22]. Interestingly, we observed significantly higher levels of the G6PD, TKT and TALDO in Post-R relative to the Post-NR, whose levels remain similar to Pre-NR (Figure 3A-3D). We also measured the levels of key pentose phosphate pathway metabolites generated using GC-MS. Sedoheptulose-7-phosphate and fructose-6-phosphate in Post-R were significantly reduced relative to Post-NR (Figure 3E and 3F). Together with potentially increased enzyme activity, this pattern could be consistent with increased non-oxidative pentose phosphate pathway flux in HF patients with clinical signs of myocardial recovery after LVAD-induced unloading.

The pentose phosphate pathway generates ribose which serves as a precursor for ribitol, that is required for glycosylation and full activity of α-dystroglycan (DAG1) [23]. The levels of ribitol was significantly higher in failing hearts relative to donors, but was significantly reduced in Post-R as compared to Post-NR with similar levels to donors (Figure 4A). Protein levels of ribitol-5-phosphate cytidylyltransferase (ISPD), which generates CDP-ribitol, a precursor for DAG1 glycosylation were decreased in the failing heart (Figure 4B and 4C). However, ISPD levels in Post-R were significantly increased relative to Post-NR (Figure 4B and 4C). Fukutin-related protein (FKRP), which mediates the addition of CDP-ribitol to DAG1, were similar between Post-NR and Post-R, but was statistically increased relative to donors, only in Post-R (Figure 4B and 4D). Moreover, western blot analysis using an antibody which specifically detects glycosylated DAG1 (referred as F-α-DAG) revealed a significantly higher level of DAG1 glycosylation in Post-R relative to Post-NR (Figure 4E and 4F). FKRP is not rate-limiting for DAG1 glycosylation, which is more dependent on

increased availability of CDP-ribitol [11, 24]. Thus overall, these results are consistent with a model in which, in responders, increased oxidative pentose phosphate pathway flux could channel ribitol and CDP-ribitol towards DAG1-glycosylation. Increased DAG1-glycosylation would be predicted to increase its activity for maintaining extracellular matrix and cytoskeletal integrity.

One-Carbon metabolism and myocardial recovery

To determine the relationship between recovery and one-carbon metabolism, we assessed key enzymes and metabolite levels in this pathway (Figure 1). Figure 5A-5C shows that the rate-limiting enzyme PHGDH, and serine hydroxymethyl transferase (SHMT) were significantly induced in Post-R relative to Post-NR. Notably, while PHGDH appears to be increasing in failing hearts, SHMT2 follows an opposite trend. Levels of serine (Figure 5D) and glycine (Figure 5E), which are intermediates in the one-carbon metabolism pathway, were significantly decreased in Post-R relative to Post-NR. Together, these changes could be consistent with increased flux through the one-carbon metabolic pathway in Post-R, suggesting an association between increased one-carbon metabolism and post-LVAD cardiac improvement in responders.

The ribose sugars generated from pentose phosphate pathway and the one-carbon metabolites from one-carbon metabolism are utilized for nucleotide synthesis. We measured the metabolite levels of various nucleobases in donors and post-LVAD responders and non-responders. Figure 5F shows significantly higher levels of nucleobases in Post-NR relative to donors and significant reduction in Post-R relative to Post-NR. One possibility accounting for the equivalent nucleobase levels between non-failing hearts and Post-R, could be increased utilization in Post-R for repair/transcription process. To determine whether decreased nucleotides in Post-R correlates with increased RNA or protein synthesis (possibly required for completion of cell cycle [25]), we quantified the ribosomal proteins L7a and S3, as an indirect measure. Figure 5G-5I shows a significant increase in both the ribosomal proteins, L7a and S3 (Figure 5H and 5I **respectively**) in Post-R as compared to Post-NR, could indicate increased usage of nucleotides in Post-R for RNA, ribosomes and ultimately protein synthesis.

Redox pathways in responders and non-responders

The NADP+/NADPH ratio reflects the redox status in the cell. NADPH, the reduced form of NADP, plays an important role in maintaining antioxidant defenses by neutralizing reactive oxygen species (ROS). We therefore analyzed the NADPH levels and ROS in the myocardial tissue. As shown in Figure 6A, NADPH levels are significantly reduced in Pre-NR and Post-NR hearts relative to donor hearts. In contrast, NADPH levels were reduced to a lesser extent in Pre-R and were not statistically different from those of donor hearts in Post-R. NADPH was significantly higher in Post-R relative to Post-NR. Consistent with this, NADP+/NADPH ratio was highest in NR regardless of pre- or post-LVAD (Figure 6B). The NADP+/NADPH ratio in pre-R hearts was similar to that of donor controls, and was maintained at that low level in Post-R subjects (Figure 6B). Thus, the NADPH pool may identify those hearts that are more likely to recover post LVAD implantation.

4-hydroxynonenal antibody (4-HNE), a highly reactive cytotoxic aldehyde released during lipid peroxidation by ROS forms stable protein-adducts and is an indirect measure of oxidative stress. There was a significant increase 4-HNE adducts in Post-NR as compared to donors. In contrast, Post-R exhibited reduced levels of 4-HNE relative to Post-NR, that were unchanged relative to donors (Figure 6C and 6D). To further confirm our results, we used the OxyBlot Protein Oxidation Detection kit to detect protein carbonylation. The pattern observed was similar to that of 4-HNE, with the highest levels of protein carbonylation seen in Post-NR and the lowest levels in Post-R (Figure 6E). Protein carbonylation was similar between non-failing donors and failing hearts at the Pre-LVAD implantation time point irrespective of the outcome post-LVAD implantation. Prior studies have suggested that LVAD induces oxidative stress in lymphocytes of HF patients [26], whether similar effects occur in cardiomyocytes remain to be demonstrated. Our data would suggest that increased NADPH may represent an important mechanism that prevents oxidative stress in post-R hearts. Also, the evidence of these adaptations was present in responders even prior to LVAD implantation. Interestingly, antioxidant enzymes such as superoxide dismutase and catalase are similar across the groups (Supplementary Figure 1A-1D) with a slight increase in Post-NR and Post-R relative to donor hearts and are therefore less likely candidates to account for the difference in oxidative stress pathways observed between responders and non-responders.

As mitochondria are targets of oxidative damage, we evaluated mitochondrial morphology and two parameters were determined. Mitochondrial volume density (V_d) was significantly reduced in Pre-NR hearts relative to the non-failing donors, whereas V_d in pre-R hearts was not statistically different as compared to donors or to Pre-NR (Figure 6F). However, Post-R, V_d was significantly increased in Post-R relative to Post-NR and achieved the same level as donor controls (Figure 6F). Mitochondrial size distribution was also examined. There was a left-ward shift in the distribution curve towards smaller mitochondria in all failing hearts pre-LVAD relative to controls, which could indicate mitochondrial fission. The distribution shifted in Post-R mitochondria to overlap with that of control donor hearts, while the distribution of Post-NR mitochondria was unchanged (Figure 6G).

DISCUSSION

Cardiac energy metabolism is complex owing to its ability to metabolize multiple substrates and channel them into multiple pathways for energy production or biosynthesis. In the present study, we provide evidence that pentose phosphate pathway and one-carbon metabolism (but not hexosamine biosynthetic pathway or polyol pathway) in responders could contributes to cardioprotection, tissue repair and facilitate recovery. We observed a significant increase in NADPH, likely through the pentose phosphate pathway and one-carbon metabolism, that could fuel biosynthetic pathways and protect the heart from oxidative stress. In addition, improved mitochondrial density and size in responders suggested salutary effects of reduced ROS and repair pathways. We also showed that metabolites such as ribitol (generated from pentose phosphate pathway) could potentially play a role in cardiac recovery by increasing glycosylation of DAG1, required for stable interactions between cardiomyocytes and the extracellular matrix. It is noteworthy that hints of these adaptations were already present in the responders before the LVAD intervention.

(as evident from our findings in their myocardial tissue at the LVAD implantation time point). Collectively, these data identify novel metabolic mechanisms emanating from non-glycolytic glucose metabolism that may promote LVAD-induced cardiac recovery (Figure 7).

In the failing heart, the relative contribution of glucose as a metabolic substrate might increase in addition to other substrates such as ketones. There is ongoing debate regarding whether this metabolic shift away from fatty acids towards glucose in the failing heart is beneficial or detrimental in the disease progression. We observed an increase in GLUT1 suggesting an LVAD-induced upregulation of glucose uptake. However, only responders appeared to channel this excess glucose to accessory pathways of glycolysis. One hallmark of increased glucose metabolism in hypertrophic hearts is accelerated glycolysis [27]. Many studies indicate that increased glycolysis is not associated with an increase in glucose oxidation suggesting an uncoupling of glycolysis and glucose oxidation [6, 28, 29]. Glucose can be metabolized in multiple pathways in addition to providing an energy source that may be more efficiently metabolized than fatty acids. These metabolites regulate multiple biological functions[27] that include potent effects on cardiomyocyte function. Our conclusions based on correlation of elevated pentose phosphate pathway and one-carbon metabolism with myocardial recovery, support an adaptive rather than maladaptive role for increased non-glycolytic glucose metabolism.

Therapeutic interventions such as LVADs and beta-blockers are increasingly suggested to modulate metabolism, which could account for their positive effects on HF patients[7, 30, 31]. We have reported previously, a post-LVAD dissociation between glycolysis and oxidative phosphorylation[7]. That study revealed that there was an increase in glycolytic intermediates, amino acids and nucleobases following LVAD-unloading relative to a match paired pre-LVAD time point, without a concomitant increase in TCA cycle and mitochondrial respiration [7]. One intriguing concept is that glycolysis though being less efficient in terms of generating ATP, the decreased myocardial energy demand during unloading or resting could make glycolysis an adequate energy source. Additionally, since most of the ROS is generated by mitochondrial respiration, the flux of glycolytic intermediates to other pathways that mediate redox homeostasis could be beneficial for the heart. This could result in reducing inexorable ROS generation as the disease progresses and may favor cardiac recovery.

The work presented here provides evidence that the glycolytic intermediates were predominantly directed towards pentose phosphate pathway and one-carbon metabolism pathways in Post-R but not in non-responders. Increased flux into these metabolic pathways in responders was also accompanied with improved mitochondrial dynamics and beneficial changes in a regulator extracellular matrix integrity. It is well established that the mitochondrial structure and dysfunction is tightly associated with ROS[32]. Aberrant mitochondrial morphology may lead to enhanced ROS formation, which, in turn could impair mitochondrial bioenergetics and damage mitochondria in other ways to further exacerbate oxidative stress in a self-perpetuating vicious cycle. Also, ROS plays a major role in the pathophysiology of HF and triggers ventricular remodeling through numerous mechanisms[33]. Of note, *G6PD-deficient* mice exhibit increased ischemia-reperfusion injury, supporting the importance of the pentose phosphate pathway in protection against oxidative

injury[34]. One hypothesis raised by the findings of this study is that increases in mitochondrial density and size could possibly be explained in part by increased generation of NADPH. Although NADPH can also be generated through TCA cycle (Malic enzyme and isocitrate dehydrogenase), the major source for cytosolic NADPH remains to be pentose phosphate pathway [35]. On the other hand, one-carbon metabolism contributes substantially to mitochondrial NADPH generation[36, 37]. We observed similar TCA cycle metabolite levels between Post-NR and Post-R (data not shown), suggesting that pentose phosphate pathway and one-carbon metabolism but not TCA cycle contributes to NADPH regeneration. This in turn reduces ROS and supports synthesis of building blocks and biomolecules which could support mitochondrial biogenesis or repair. However, it is possible that increase in NADPH or functional myocardial recovery is secondary to improved mitochondrial structure and function by yet unknown mechanisms. The significantly higher nucleotide levels in Post-NR could reflect mitochondrial and nuclear DNA damage along with reduced DNA repair mechanisms and diminished transcription. Prior studies have reported that majority of cardiomyocytes in failing heart harbor a polyploid genome. A post-LVAD increase in cardiomyocyte diploidy due to cell cycle progression with mitotic cytokinesis and its correlation with recovery has been described[25].

Increased polyol pathway flux has been associated with cardiac dysfunction and reducing flux via ALDR inhibition was shown to improve cardiac functions[38, 39]. Thus, reduced glucose metabolism through the polyol pathway could also contribute to cardiac recovery. Reduced generation of sorbitol in Post-R is consistent with reduced polyol pathway flux. In addition, overexpression of the human form of ALDR in mice was found to be associated with impaired functional recovery after ischemia [39]. Similarly, repression of the hexosamine biosynthetic pathway in Post-R, could represent a protective mechanism, in light of evidence linking increased glycosylation (end-product of hexosamine biosynthetic pathway) with cardiac dysfunction [40, 41]. We also observed low O-GlcNAcylation in Post-R despite similar GFAT1 levels to Post-NR. GFAT is regulated by multiple phosphorylation events which regulates the enzyme activity [42, 43], hence it is possible that phosphorylation at specific sites might be different, however phospho-specific antibodies are not currently available. Increased O-GlcNAcylation is associated with cardiomyocyte dysfunction and reduced sarcoplasmic reticulum Ca^{+2}-ATPase expression and abnormal calcium transients [40, 41]. Additionally, glycosylation is linked to increased apoptosis [44]. On the contrary, an increased flux of glucose into hexosamine biosynthetic pathway and polyol pathway in Post-NR could possibly explain the lack of functional recovery and further progression of disease in this subset of HF patients.

Mechanical stress due to pressure and volume overload in concert with metabolic dysfunction also induces profound changes in extracellular matrix composition that contribute to the pathogenesis of HF[45]. Because of its importance in preserving structural integrity and function of the heart and its central involvement in regulating cellular responses to cardiac injury, repair, and remodeling, the cardiac extracellular matrix provides unique opportunities for therapeutic interventions in HF patients. DAG1 is an important component of extracellular matrix which is highly glycosylated with multiple ribitol-5-phosphate molecules. This glycosylation is critical for maintaining matrix and myocyte communication, essential for optimal integrity and function of muscle[11, 12, 46]. Lack of

DAG1 glycosylation results in progressive degeneration of cardiac muscles, ultimately leading to heart failure [47, 48]. Pentose phosphate pathway intermediates are the principal source of ribitol and hence for glycosylation of DAG1. Overexpression of ISPD increased ribitol incorporation into DAG1[24]. In another study, treatment of FKRP-mutant mice with ribitol increased DAG1 glycosylation levels in cardiac muscles and reduced cardiac fibrosis[11]. Our results revealed low ribitol levels in Post-R, possibly indicating enhanced utilization for DAG1 glycosylation and in support, an increase in ISPD and DAG1 glycosylation levels. We also recently announced that Post-R have significantly reduced myocardial fibrosis in contrast to Post-NR[49]. Our results also support previous reports, that F-α-DAG is critical for myocardial structure and that enhanced glycosylation of DAG1 could lead to improvement of structure and function among responders following LVAD unloading.

We provide insights into the potential mechanisms by which the failing heart undergoes functional recovery upon mechanical unloading. Studies using transgenic mouse models and pharmacological compounds have demonstrated that increased glucose metabolism in adult heart is not harmful and can be beneficial when it provides sufficient fuel for oxidative metabolism[27]. We now provide evidence for previously incompletely understood issues linking mismatch between enhanced glycolysis and reduced glucose oxidation to recovery by demonstrating that non-glycolytic pathways of glucose metabolism are induced specifically in HF patients with improved myocardial function. These pathways could promote cardioprotection by improving redox homeostasis, reducing oxidative stress, enhancing mitochondrial structural integrity, and restoring extracellular matrix function (Figure 7). Together these observations point to a potentially favorable benefit of the metabolic shift to glucose in the failing heart specifically in responders. However, this sole metabolic shift does not necessarily mean adaptive and there might be multiple other metabolic/signaling pathways at play.

Study limitations:

HF is a complex disease with multiple factors responsible for the disease etiology, it will be inappropriate to confine glucose metabolism as solely responsible for cardiac recovery. There are likely other important metabolic pathways that were not tested. Furthermore, our metabolomics data represents static levels of metabolites, thus, future studies using C^{13}-glucose flux might distinctly reveal the precise pathways of glucose metabolism in HF. Finally, there were likely variable populations of cells other than cardiomyocytes such as fibroblasts and macrophages in the tissue used which can influence the results, that are beyond the scope of this study and could be addressed in future using single cell approaches.

In conclusion, the recovering heart appears to direct glycolytic metabolites into pentose phosphate pathway and one-carbon metabolism which could contribute to cardioprotection by generating NADPH to enhance biosynthesis and to cope with oxidative stress. A better understanding of metabolic changes occurring in the failing and recovering heart would be helpful in developing metabolic therapies. Interventions that enhance glucose flux into cardioprotective pathways potentially improve the mitochondrial or extracellular matrix dynamics and should be investigated further as a strategy to enhance myocardial recovery.

Supplementary Material

Refer to Web version on PubMed Central for supplementary material.

ACKNOWLEDGEMENTS:

The authors are grateful to DonorConnect for facilitating the access of our team to myocardial tissue from patients that donated their hearts for research purposes (DonorConnect is a federally designated, nonprofit community service organization dedicated to the recovery and transplantation of organs and tissues for Utah, southeastern Idaho, western Wyoming, and Elko, Nevada). The authors thank Dr. James Cox for performing metabolomics analysis, Dr. Timothy Parnell for performing bioinformatics analysis on RNA sequencing data and Ms. Diana Lim for helping with the graphical abstract for the manuscript. The authors also thank members of our research team for collecting myocardial tissue and blood from HF patients and donors.

Dr. Drakos certify that (1) all persons who have made substantial contributions to the manuscript (e.g., data collection, analysis, or writing or editing assistance), but who do not fulfill authorship criteria, are named with their specific contributions in the Acknowledgments section of the manuscript; (2) all persons named in the Acknowledgments section have provided the corresponding author with written permission to be named in the manuscript; and (3) if an Acknowledgments section is not included, no other persons besides the authors have made substantial contributions to this manuscript.

SOURCES OF FUNDING

This work was supported by American Heart Association- Heart Failure Strategically Focused Research Network, Grant 16SFRN29020000 (Drs. Selzman, Drakos, and Abel); National Heart, Lung and Blood Institute (NHLBI) RO1 Grant HL135121 (Dr. Drakos); NHLBI RO1 Grant HL132067 (Dr. Drakos) and; American Heart Association Post-doctoral fellowship 19POST34381084 (Dr. Badolia). Additional support was provided by the Nora Eccles Treadwell Foundation to Drs. Rutter and Drakos. Dr. Rutter also receives support from Howard Hughes Medical Institute.

Non-standard Abbreviations and Acronyms:

LVAD	Left Ventricular Assist Devices
HF	Heart Failure
R	Responder
NR	Non-responder
LVEF	Left Ventricular Ejection Fraction
LVEDD	Left Ventricular End Diastolic Diameter
GC-MS	Gas chromatography-mass spectrometry
TCA	Tricarboxylic acid cycle
ROS	Reactive oxygen species
HSP60	Heat shock protein 60
GLUT	Glucose transporters
GFAT1	Glutamine fructose-6-phosphate amidotransferase 1
UDPGlcNAc	Uridine diphosphate-N-acetylglucosamine
ALDR	Aldose reductase

G6PD	Glucose-6-phosphate dehydrogenase
TKT	Transketolase
TALDO	Transaldolase
DAG1	alpha-Dystroglycan
F-α-DAG	glycosylated DAG1
ISPD	D-Ribitol-5-phosphate cytidylyltransferase
FKRP	Fukutin-related protein
PHGDH	Phosphoglycerate dehydrogenase
SHMT2	Serine Hydroxymethyl transferase 2
4-HNE	4-hydroxynonenal antibody

REFERENCES

1. Drakos SG, Terrovitis JV, Anastasiou-Nana MI and Nanas JN. Reverse remodeling during long-term mechanical unloading of the left ventricle. J Mol Cell Cardiol. 2007;43:231–242. [PubMed: 17651751]
2. Drakos SG, Wever-Pinzon O, Selzman CH, Gilbert EM, Alharethi R, Reid BB, Saidi A, Diakos NA, Stoker S, Davis ES and et al. Magnitude and time course of changes induced by continuous-flow left ventricular assist device unloading in chronic heart failure: insights into cardiac recovery. J Am Coll Cardiol. 2013;61:1985–1994. [PubMed: 23500219]
3. Drakos SG and Mehra MR. Clinical myocardial recovery during long-term mechanical support in advanced heart failure: Insights into moving the field forward. J Heart Lung Transplant. 2016;35:413–420. [PubMed: 26922277]
4. Jaswal JS, Keung W, Wang W, Ussher JR and Lopaschuk GD. Targeting fatty acid and carbohydrate oxidation--a novel therapeutic intervention in the ischemic and failing heart. Biochimica et biophysica acta. 2011;1813:1333–1350. [PubMed: 21256164]
5. Huss JM and Kelly DP. Mitochondrial energy metabolism in heart failure: a question of balance. J Clin Invest. 2005;115:547–555. [PubMed: 15765136]
6. Allard MF, Schonekess BO, Henning SL, English DR and Lopaschuk GD. Contribution of oxidative metabolism and glycolysis to ATP production in hypertrophied hearts. Am J Physiol. 1994;267:H742–H750. [PubMed: 8067430]
7. Diakos NA, Navankasattusas S, Abel ED, Rutter J, McCreath L, Ferrin P, McKellar SH, Miller DV, Park SY, Richardson RS and et al. Evidence of Glycolysis Up-Regulation and Pyruvate Mitochondrial Oxidation Mismatch During Mechanical Unloading of the Failing Human Heart: Implications for Cardiac Reloading and Conditioning. JACC Basic Transl Sci. 2016;1:432–444. [PubMed: 28497127]
8. Chokshi A, Drosatos K, Cheema FH, Ji R, Khawaja T, Yu S, Kato T, Khan R, Takayama H, Knoll R and et al. Ventricular assist device implantation corrects myocardial lipotoxicity, reverses insulin resistance, and normalizes cardiac metabolism in patients with advanced heart failure. Circulation. 2012;125:2844–2853. [PubMed: 22586279]
9. Gupte AA, Hamilton DJ, Cordero-Reyes AM, Youker KA, Yin Z, Estep JD, Stevens RD, Wenner B, Ilkayeva O, Loebe M and et al. Mechanical unloading promotes myocardial energy recovery in human heart failure. Circ Cardiovasc Genet. 2014;7:266–276. [PubMed: 24825877]
10. Barcia-Vieitez R and Ramos-Martinez JI. The regulation of the oxidative phase of the pentose phosphate pathway: new answers to old problems. IUBMB life. 2014;66:775–779. [PubMed: 25408203]

11. Cataldi MP, Lu P, Blaeser A and Lu QL. Ribitol restores functionally glycosylated α-dystroglycan and improves muscle function in dystrophic FKRP-mutant mice. Nat Commun. 2018;9:3448. [PubMed: 30150693]
12. Yoshida-Moriguchi T and Campbell KP. Matriglycan: a novel polysaccharide that links dystroglycan to the basement membrane. Glycobiology. 2015;25:702–713. [PubMed: 25882296]
13. Fan J, Ye J, Kamphorst JJ, Shlomi T, Thompson CB and Rabinowitz JD. Quantitative flux analysis reveals folate-dependent NADPH production. Nature. 2014;510:298–302. [PubMed: 24805240]
14. Ducker GS and Rabinowitz JD. One-Carbon Metabolism in Health and Disease. Cell metab. 2017;25:27–42. [PubMed: 27641100]
15. Wever-Pinzon J, Selzman CH, Stoddard G, Wever-Pinzon O, Catino A, Kfoury AG, Diakos NA, Reid BB, McKellar S, Bonios M and et al. Impact of Ischemic Heart Failure Etiology on Cardiac Recovery During Mechanical Unloading. J Am Coll Cardiol. 2016;68:1741–1752. [PubMed: 27737740]
16. Szablewski L Glucose transporters in healthy heart and in cardiac disease. Int J Cardiol. 2017;230:70–75. [PubMed: 28034463]
17. Yang J, Moravec CS, Sussman MA, DiPaola NR, Fu D, Hawthorn L, Mitchell CA, Young JB, Francis GS, McCarthy PM and et al. Decreased SLIM1 expression and increased gelsolin expression in failing human hearts measured by high-density oligonucleotide arrays. Circulation. 2000;102:3046–3052. [PubMed: 11120693]
18. Wells L, Vosseller K and Hart GW. Glycosylation of nucleocytoplasmic proteins: signal transduction and O-GlcNAc. Science (New York, NY). 2001;291:2376–2378.
19. Young ME, Yan J, Razeghi P, Cooksey RC, Guthrie PH, Stepkowski SM, McClain DA, Tian R and Taegtmeyer H. Proposed regulation of gene expression by glucose in rodent heart. Gene Regul Syst Biol. 2007;1:251–262.
20. Watson LJ, Facundo HT, Ngoh GA, Ameen M, Brainard RE, Lemma KM, Long BW, Prabhu SD, Xuan YT and Jones SP. O-linked beta-N-acetylglucosamine transferase is indispensable in the failing heart. Proc Nat Acad Sci USA. 2010;107:17797–17802. [PubMed: 20876116]
21. Zimmer HG. Regulation of and intervention into the oxidative pentose phosphate pathway and adenine nucleotide metabolism in the heart. Mol cell biochem. 1996;160–161:101-109.
22. Meerson FZ, Spiritchev VB, Pshennikova MG and Djachkova LV. The role of the pentose-phosphate pathway in adjustment of the heart to a high load and the development of myocardial hypertrophy. Experientia. 1967;23:530–532. [PubMed: 4228586]
23. Toivari MH, Maaheimo H, Penttila M and Ruohonen L. Enhancing the flux of D-glucose to the pentose phosphate pathway in Saccharomyces cerevisiae for the production of D-ribose and ribitol. Appl microbiol biotechnol. 2010;85:731–739. [PubMed: 19711072]
24. Gerin I, Ury B, Breloy I, Bouchet-Seraphin C, Bolsee J, Halbout M, Graff J, Vertommen D, Muccioli GG, Seta N and et.al. ISPD produces CDP-ribitol used by FKTN and FKRP to transfer ribitol phosphate onto alpha-dystroglycan. Nat Commun. 2016;7:11534. [PubMed: 27194101]
25. Wohlschlaeger J, Levkau B, Brockhoff G, Schmitz KJ, von Winterfeld M, Takeda A, Takeda N, Stypmann J, Vahlhaus C, Schmid C and et al. Hemodynamic support by left ventricular assist devices reduces cardiomyocyte DNA content in the failing human heart. Circulation. 2010;121:989–996. [PubMed: 20159834]
26. Mondal NK, Sorensen E, Hiivala N, Feller E, Griffith B and Wu ZJ. Oxidative stress, DNA damage and repair in heart failure patients after implantation of continuous flow left ventricular assist devices. Int J Med Sci. 2013;10:883–893. [PubMed: 23781134]
27. Kolwicz SC, Jr. and Tian R. Glucose metabolism and cardiac hypertrophy. Cardiovasc Res. 2011;90:194–201. [PubMed: 21502371]
28. Wambolt RB, Henning SL, English DR, Dyachkova Y, Lopaschuk GD and Allard MF. Glucose utilization and glycogen turnover are accelerated in hypertrophied rat hearts during severe low-flow ischemia. J mol cell cardiol. 1999;31:493–502. [PubMed: 10198181]
29. El Alaoui-Talibi Z, Guendouz A, Moravec M and Moravec J. Control of oxidative metabolism in volume-overloaded rat hearts: effect of propionyl-L-carnitine. Am J physiol. 1997;272:H1615–H1624. [PubMed: 9139943]

30. Eichhorn EJ, Heesch CM, Barnett JH, Alvarez LG, Fass SM, Grayburn PA, Hatfield BA, Marcoux LG and Malloy CR. Effect of metoprolol on myocardial function and energetics in patients with nonischemic dilated cardiomyopathy: a randomized, double-blind, placebo-controlled study. J Am Coll Cardiol. 1994;24:1310–1320. [PubMed: 7930255]

31. Beanlands RS, Nahmias C, Gordon E, Coates G, deKemp R, Firnau G and Fallen E. The effects of beta(1)-blockade on oxidative metabolism and the metabolic cost of ventricular work in patients with left ventricular dysfunction: A double-blind, placebo-controlled, positron-emission tomography study. Circulation. 2000;102:2070–2075. [PubMed: 11044422]

32. Tsushima K, Bugger H, Wende AR, Soto J, Jenson GA, Tor AR, McGlauflin R, Kenny HC, Zhang Y, Souvenir R and et al. Mitochondrial Reactive Oxygen Species in Lipotoxic Hearts Induce Post-Translational Modifications of AKAP121, DRP1, and OPA1 That Promote Mitochondrial Fission. Circ Res. 2018;122:58–73. [PubMed: 29092894]

33. Gupte SA, Levine RJ, Gupte RS, Young ME, Lionetti V, Labinskyy V, Floyd BC, Ojaimi C, Bellomo M, Wolin MS and et al. Glucose-6-phosphate dehydrogenase-derived NADPH fuels superoxide production in the failing heart. J Mol cell cardiol. 2006;41:340–349. [PubMed: 16828794]

34. Jain M, Cui L, Brenner DA, Wang B, Handy DE, Leopold JA, Loscalzo J, Apstein CS and Liao R. Increased myocardial dysfunction after ischemia-reperfusion in mice lacking glucose-6-phosphate dehydrogenase. Circulation. 2004;109:898–903. [PubMed: 14757696]

35. Chen L, Zhang Z, Hoshino A, Zheng HD, Morley M, Arany Z and Rabinowitz JD. NADPH production by the oxidative pentose-phosphate pathway supports folate metabolism. Nat metab. 2019;1:404–415.

36. Lewis CA, Parker SJ, Fiske BP, McCloskey D, Gui DY, Green CR, Vokes NI, Feist AM, Vander Heiden MG and Metallo CM. Tracing compartmentalized NADPH metabolism in the cytosol and mitochondria of mammalian cells. Molecular cell. 2014;55:253–263. [PubMed: 24882210]

37. Ducker GS, Chen L, Morscher RJ, Ghergurovich JM, Esposito M, Teng X, Kang Y and Rabinowitz JD. Reversal of Cytosolic One-Carbon Flux Compensates for Loss of the Mitochondrial Folate Pathway. Cell metab. 2016;23:1140–1153. [PubMed: 27211901]

38. Johnson BF, Nesto RW, Pfeifer MA, Slater WR, Vinik AI, Chyun DA, Law G, Wackers FJ and Young LH. Cardiac abnormalities in diabetic patients with neuropathy: effects of aldose reductase inhibitor administration. Diabetes care. 2004;27:448–454. [PubMed: 14747227]

39. Hwang YC, Kaneko M, Bakr S, Liao H, Lu Y, Lewis ER, Yan S, Ii S, Itakura M, Rui L and et al. Central role for aldose reductase pathway in myocardial ischemic injury. FASEB J. 2004;18:1192–1199. [PubMed: 15284219]

40. Clark RJ, McDonough PM, Swanson E, Trost SU, Suzuki M, Fukuda M and Dillmann WH. Diabetes and the accompanying hyperglycemia impairs cardiomyocyte calcium cycling through increased nuclear O-GlcNAcylation. J biol chem. 2003;278:44230–44237. [PubMed: 12941958]

41. Hu Y, Belke D, Suarez J, Swanson E, Clark R, Hoshijima M and Dillmann WH. Adenovirus-mediated overexpression of O-GlcNAcase improves contractile function in the diabetic heart. Circ res. 2005;96:1006–1013. [PubMed: 15817886]

42. Chang Q, Su K, Baker JR, Yang X, Paterson AJ and Kudlow JE. Phosphorylation of human glutamine:fructose-6-phosphate amidotransferase by cAMP-dependent protein kinase at serine 205 blocks the enzyme activity. J biol chem. 2000;275:21981–21987. [PubMed: 10806197]

43. Li Y, Roux C, Lazereg S, LeCaer JP, Laprevote O, Badet B and Badet-Denisot MA. Identification of a novel serine phosphorylation site in human glutamine:fructose-6-phosphate amidotransferase isoform 1. Biochemistry. 2007;46:13163–13169. [PubMed: 17941647]

44. Fiordaliso F, Leri A, Cesselli D, Limana F, Safai B, Nadal-Ginard B, Anversa P and Kajstura J. Hyperglycemia activates p53 and p53-regulated genes leading to myocyte cell death. Diabetes. 2001;50:2363–2375. [PubMed: 11574421]

45. Frangogiannis NG. The extracellular matrix in myocardial injury, repair, and remodeling. J clin invest. 2017;127:1600–1612. [PubMed: 28459429]

46. Sheikh MO, Halmo SM and Wells L. Recent advancements in understanding mammalian O-mannosylation. Glycobiology. 2017;27:806–819. [PubMed: 28810660]

47. Brockington M, Yuva Y, Prandini P, Brown SC, Torelli S, Benson MA, Herrmann R, Anderson LV, Bashir R, Burgunder JM and et al. Mutations in the fukutin-related protein gene (FKRP) identify limb girdle muscular dystrophy 2I as a milder allelic variant of congenital muscular dystrophy MDC1C. Hum mol genet. 2001;10:2851–2859. [PubMed: 11741828]

48. Brown SC, Torelli S, Brockington M, Yuva Y, Jimenez C, Feng L, Anderson L, Ugo I, Kroger S, Bushby K and et al. Abnormalities in alpha-dystroglycan expression in MDC1C and LGMD2I muscular dystrophies. Am j pathol. 2004;164:727–737. [PubMed: 14742276]

49. Ferrin P, McCreath L, Diakos N, Navankasattusas S, Kfoury AG, Wever-Pinzon O, Al-Sarie M, Catino A, Bonios M, Alharethi R and et al. (11) - Relationship of Myocardial Fibrosis with the Potential of Mechanical Unloading to Induce Favorable Cardiac Structural and Functional Response. J Heart Lung Transplant. 2016;35:S12–S13.

CLINICAL PERSPECTIVE:

What is new?:

- Our study demonstrates that increase in non-glycolytic pathways of glucose metabolism involved in NADPH production and biosynthesis, correlates with cardiac recovery in LVAD-unloaded HF patients.

What are the clinical implications?

- This new information could redirect future translational investigations in an effort to identify novel therapeutic targets for myocardial recovery in chronic HF patients.

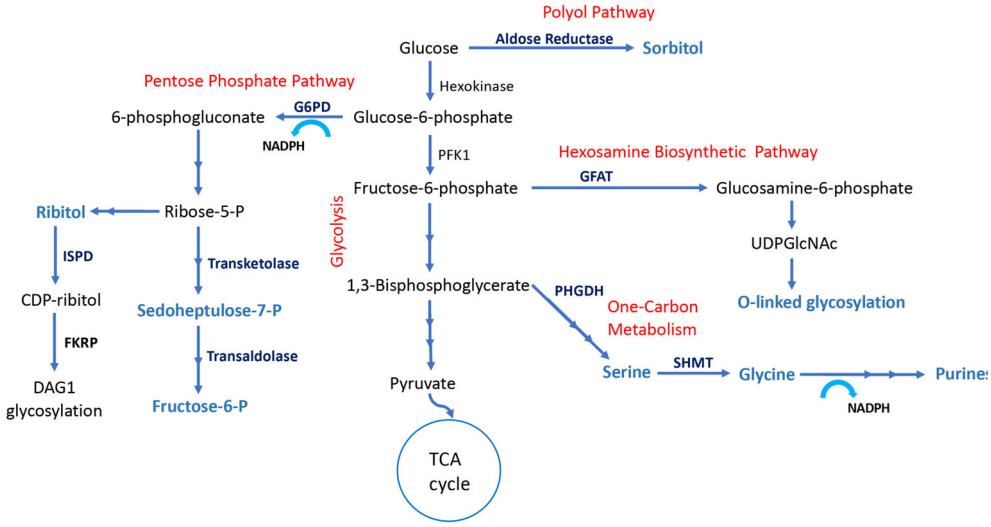

Figure 1: Accessory pathways of glucose metabolism:

Glucose is converted to glucose-6-phosphate once it enters the cell via glucose transporters (GLUT1 and GLUT4). Glucose can be oxidized via glycolysis to pyruvate which enters TCA cycle in mitochondria to complete glucose oxidation. Alternatively, glucose can enter into polyol pathway and converted to sorbitol via rate-limiting aldose reductase (ALDR) enzyme. Glucose-6-P can be channeled into Pentose Phosphate pathway by rate-limiting glucose-6-phosphate dehydrogenase (G6PD), generating pentose sugars for nucleotide synthesis and NADPH. Pentose sugar, ribose generated from the pentose phosphate pathway is converted to ribitol and subsequently to CDP-ribitol by ribitol-5-phosphate cytidylyltransferase (ISPD), and is conjugated with α-dystroglycan (DAG1) as a glycosylation motif by fukutin-related protein (FKRP) enzyme. Fructose-6-phophate, a glycolytic intermediate can be channeled into the hexosamine biosynthetic pathway by rate-limiting glutamine fructose-6-phosphate amidotransferase (GFAT) and converted to UDP-GlcNAc used for glycosylation of proteins. Additionally, glycolytic intermediate 3-phosphoglycerate enters one-carbon metabolism pathway by the rate-limiting, phosphoglycerate dehydrogenase (PHGDH) and among other steps, interconversion of glycine and serine by serine hydroxymethyl transferase (SHMT), thereby generating one-carbon units for nucleotide and NADPH synthesis.

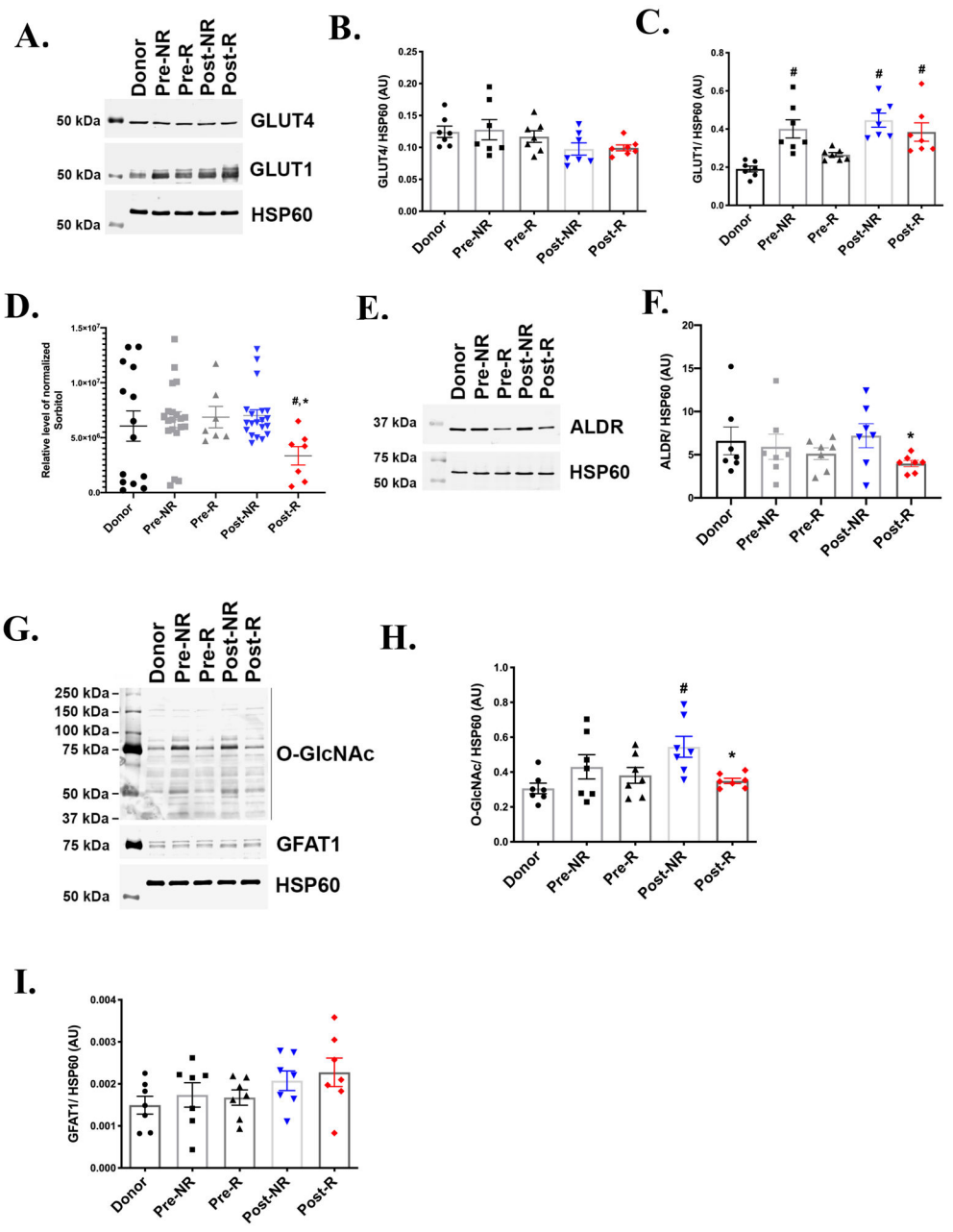

Figure 2: Glucose uptake, Polyol and Hexosamine biosynthetic pathways.

A) Representative western blot from 7 independent experiments, showing the protein levels of glucose transporters 1 and 4 (GLUT1 and GLUT 4) in paired responders (R) and non-responders (NR) derived pre- and post-LVAD myocardial samples. Donors serves as the non-failing control and heat shock protein 60 (HSP60) is the lane loading control. Densitometric analysis of the western blots normalized to HSP60 showing similar levels of **(B)** GLUT4 and **(C)** GLUT1 in Post-R as compared to Post-NR. (n=7 for each group). **D)** Gas chromatography-mass spectrometry (GC-MS) analysis of myocardial tissue samples across the groups showing significantly reduced sorbitol levels in Post-R (n= donors-14, NR-20, R-7). **E-F)** Representative western blot and corresponding densitometric analysis for

enzyme aldose reductase (ALDR). **G)** Representative western blot and corresponding densitometric analysis for hexosamine biosynthetic pathway **H)** rate-limiting enzyme, glutamine fructose-6-phosphate amidotransferase1 (GFAT1) and **I)** O-GlcNAcylation. p-value < 0.05 was considered significant; # $p < 0.05$ as compared to donors; * $p < 0.05$ compared to Post-NR. Error bars represent standard error of mean (SEM).

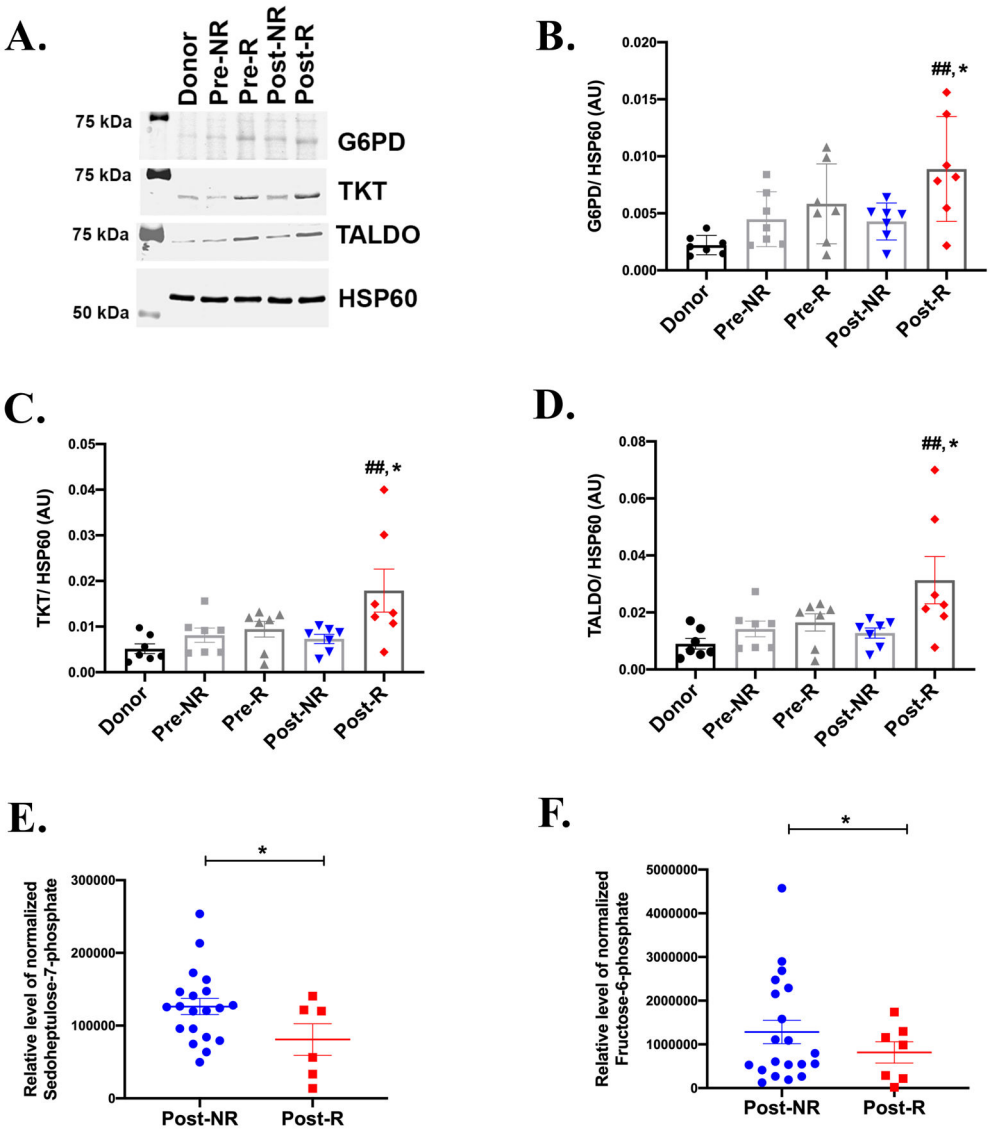

Figure 3: Pentose phosphate pathway-associated myocardial recovery in HF patients.

A) Representative western blot from 7 independent experiments, showing the protein levels of glucose-6-phosphate dehydrogenase (G6PD), transaldolase (TALDO) and transketolase (TKT) in paired responders (R) and non-responders (NR). HSP60 is the lane loading control. Densitometric analysis of the western blots normalized to HSP60 showing significantly enhanced levels of **(B)** G6PD, **(C)** TKT and **(D)** TALDO in Post-R as compared to Post-NR. (n=7 for each group). GC-MS analysis of myocardial tissue samples showing reduced levels of metabolic substrates **E)** sedoheptulose-7-phosphate and **F)** fructose-6-phosphate in Post-R (n=donors-14, NR-20, R-7). p-value < 0.05 was considered significant; ##p<0.01 as compared to donors; *p< 0.05 compared to Post-NR. Error bars represent SEM.

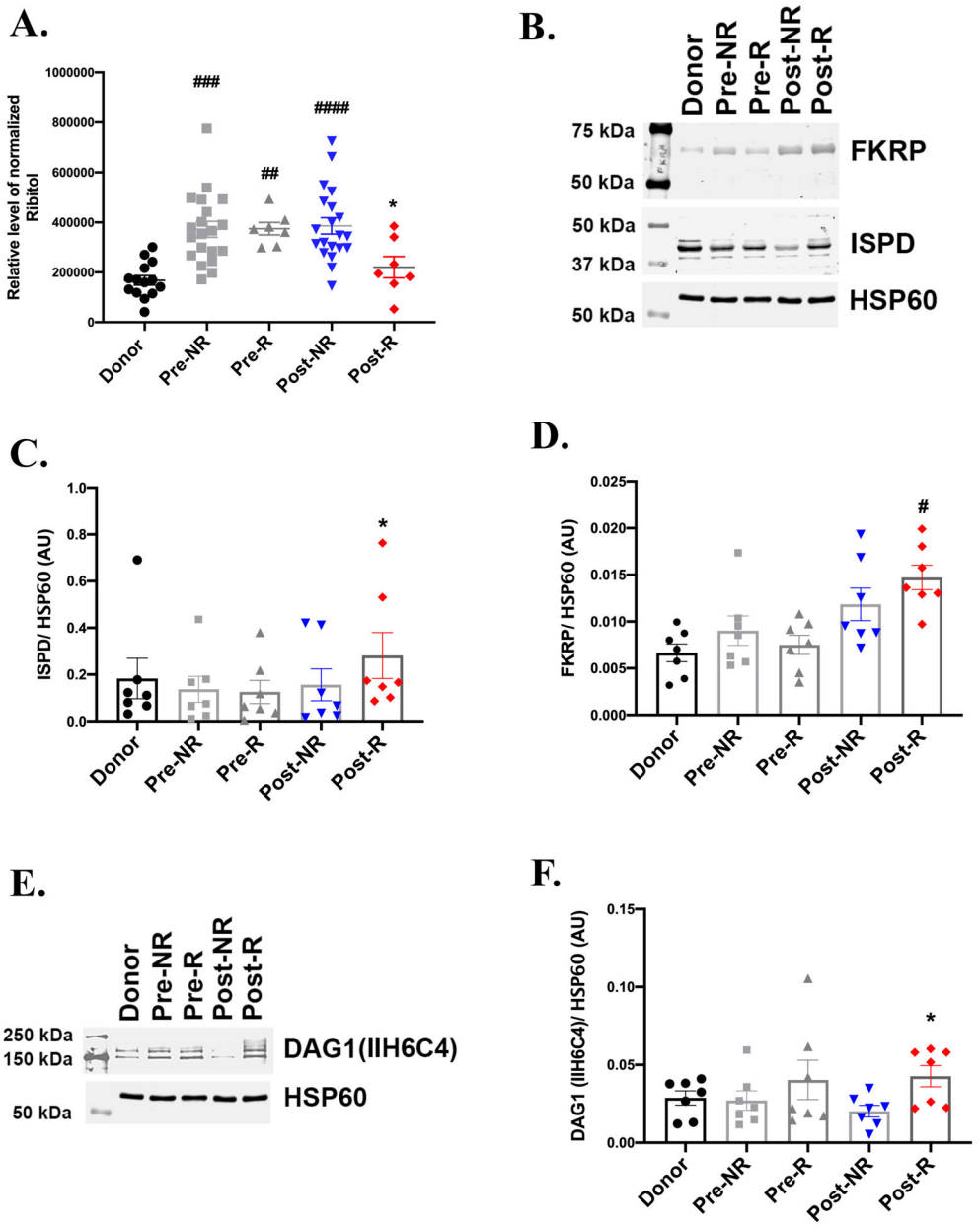

Figure 4: Enhanced α-dystroglycan glycosylation correlates with myocardial recovery.

A) GC-MS analysis depicts similar levels of ribitol in donor and Post-R, with an increase in non-failing heart and Post-NR (n= donors-14, NR-20, R-7). **B)** Representative western blot from 7 independent experiments revealing enhanced levels of ribitol-5-phosphate cytidylyltransferase (ISPD) and similar fukutin-related protein (FKRP) protein levels in Post-R as compared to Post-NR. HSP60 is the lane loading control. **C**) and **D)** Densitometric analysis normalized to HSP60 of the western blots for ISPD and FKRP respectively. **E**) Representative western blot and **F)** corresponding densitometric analysis, showing enhanced glycosylation of α-dystroglycan (DAG1) in Post-R. n=7 for each group; p-value < 0.05 was considered significant; #p< 0.05, ##p<0.01, ###p<0.001 and ####p<0.0001 as compared to donors; *p< 0.05 compared to Post-NR.

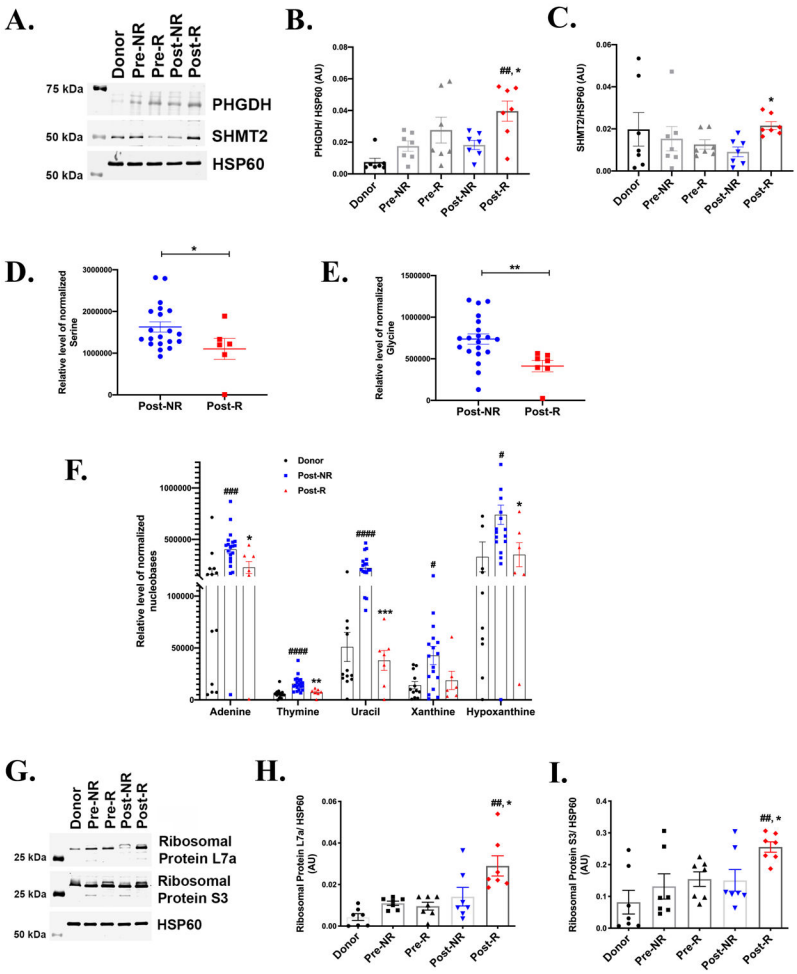

Figure 5: One-Carbon metabolism and myocardial recovery.

A) Representative western blot from 7 independent experiments, showing the protein levels of phosphoglycerate dehydrogenase (PHGDH) and serine hydroxymethyl transferase 2 (SHMT2) in paired responders (R) and non-responders (NR). Donors serve as the non-failing control and HSP60 is the lane loading control. Densitometric analysis normalized to HSP60 of the western blots showing significantly enhanced levels of **(B)** PHGDH and **(C)** SHMT2 in Post-R as compared to Post-NR. (n=7 for each group). Error bars represent SEM. GC-MS analysis of myocardial tissue samples across the groups showing reduced levels of metabolic substrates **D)** serine and **E)** glycine (n= donors-14, NR-20, R-7). **F)** Metabolite levels of various nucleotides (n= donors-14, NR-20, R-7). **G)** Representative western blot of ribosomal proteins and corresponding densitometric analysis of **H)** Ribosomal protein S3 and **I)** Ribosomal protein L7a (n=7 for each group). p-value < 0.05 was considered significant; #p< 0.05, ##p< 0.01, ###p< 0.001 and ####p<0.0001 as compared to donors; *p< 0.05, **p<0.01, ***p<0.001 compared to Post-NR.

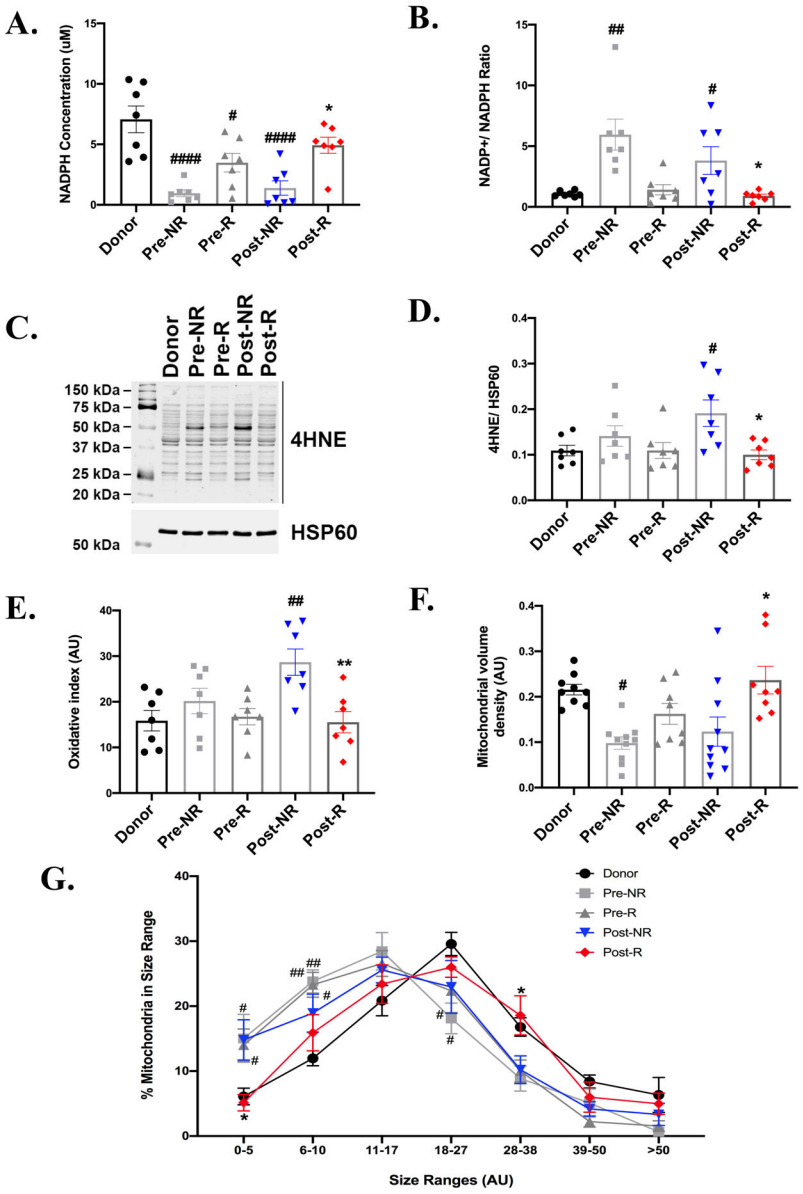

Figure 6: Oxidative stress and mitochondrial adaptations to increased non-glycolytic glucose metabolism.

A. NADPH levels and **B)** NADP+/NADPH ratio measured using the NADP+/ NADPH kit shows high NADPH levels and reduced ratio in Post-R. **C)** and **D)** Representative western blot and densitometric analysis from 7 independent experiments showing using 4-hydroxynonenal (4-HNE) oxidative modifications in paired tissue samples from pre- and Post-Responders (R) and non-responders (NR). HSP60 is the lane loading control. **E)** Graph showing densitometric analysis of the reactive oxygen species (ROS) modifications revealed using the oxy-blot detection kit. (n=7 for each group). **F)** Mitochondrial volume density and **G)** mitochondria size range using electron microscopy images. (n= donors-5, pre and post R-7, pre and post NR-7). p-value < 0.05 was considered significant; #p< 0.05, ##p<0.01 and ####p<0.0001 as compared to donors; *p< 0.05 and **p<0.01 compared to Post-NR. Error bars represent SEM.

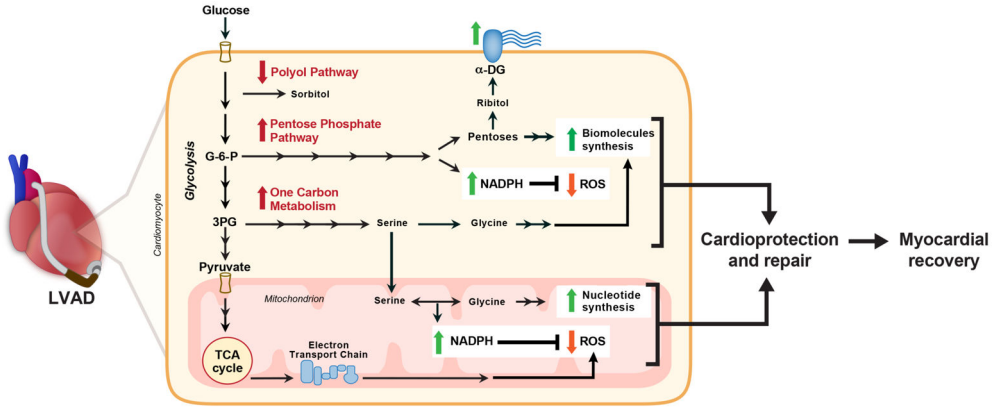

Figure 7: Model for non-oxidative pathways of glucose metabolism derived from glycolytic intermediates in LVAD-induced cardiac recovery.

The cardiac recovery in responders following LVAD-induced mechanical unloading correlates with an increased flux of glucose into accessory pathways such as pentose phosphate pathway and one-carbon metabolism for generation of biomolecules for repair, improving extracellular matrix integrity via α-dystroglycan glycosylation and via generation of NADPH, which is predominantly used for biosynthesis and less likely for reducing reactive oxygen species (ROS). Also, reduced flux into polyol pathway and hexosamine biosynthetic pathway appears to be beneficial.

Table 1:
Clinical Characteristics of the study population.

Left ventricular ejection fraction (LVEF) and left ventricular end diastolic diameter (LVEDD) at both LVAD implantation (pre-LVAD) and LVAD explantation/cardiac transplantation (post-LVAD) showing clinical differences between Responders and Non-Responders. (Values reported as Mean ± SEM).

Variable	Responders N=11 (mean ± SE)	Non-responders N=30 (mean ± SE)	p-value
Male sex, n (%)	9 (81.8)	26 (86.6)	0.65
Age at LVAD implantation, months	46.2±6.2	52±2.2	0.28
Pre-LVAD			
LVEDD, cm	6.2±0.4	6.8±0.2	0.24
LVEF, %	20.2±2.3	18.4±1	0.41
Post-LVAD			
LVEDD, cm	4.8±0.4	6.3±0.2	<0.001
LVEF, %	42.2±2	19.3±1	<0.001
HF Etiology			0.72
Ischemic cardiomyopathy, n (%)	3 (27.3)	12 (40.0)	
Non-ischemic cardiomyopathy, n (%)	8 (72.7)	18 (60.0)	
New York Heart Association Functional Class			0.99
II, n (%)	0 (0.0)	1 (3.3)	
III, n (%)	3 (27.3)	9 (30.0)	
IV, n (%)	8 (72.7)	10 (66.7)	
LVAD Type			0.32
HeartMate II™, n (%)	5 (45.5)	12 (40.0)	
HeartWare®, n (%)	5 (45.5)	14 (46.7)	
Jarvik 2000®, n (%)	0 (0.0)	4 (13.3)	
Levacor™, n (%)	1 (9.0)	0 (0.0)	
Duration of HF symptoms, months	53.1±23.6	121±21	0.07
Systolic Blood Pressure, mmHg	107.2±4	100±2.7	0.14
Diastolic Blood Pressure, mmHg	63±4.4	67.4±2	0.31
Mean Right Atrial Pressure, mmHg	13.5±2.5	11.2±1	0.3
Systolic Pulmonary Artery Pressure, mmHg	49.3±4	52±2.3	0.58
Diastolic Pulmonary Artery Pressure, mmHg	25.4±2.4	25.6±1.5	0.95
Pulmonary Capillary Wedge Pressure, mmHg	22±2	26±3	0.49
Cardiac Index, l/min/m^2	2±0.2	1.7±0.1	0.08
Pulmonary Vascular Resistance, Wood units	2.7±0.3	3.5±0.4	0.26
B-type Natriuretic Peptide, pg/mL	1406.6±352.3	1235±248.3	0.69
Creatinine, mg/dL	1.1±0.1	1.2±0.1	0.15
Sodium, mmol/L	133.4±2	133±1	0.85
Hemoglobin, g/dL	12.2±1	12.5±0.4	0.77